Preprints (www.preprints.org) | NOT PEER-REVIEWED | Posted: 11 June 2021 doi:10.20944/preprints202106.0327.v1

ENVIRONMENTAL ENRICHMENT AND FLUOXETINE NEUROGENIC STIMULI INCREASE ß3-TUBULIN IMMATURE NEURONS IN MENINGES THROUGH TRKB-MEDIATED SIGNALING

S. Zorzin (1), A. Corsi (1), A. Pino (1), A. Amenta (2), G. F. Fumagalli (1), C. Chiamulera (1), F. Bifari (2), I. Decimo *(1).

Affiliation:
(1) Department of Diagnostic and Public Health, Sect. of Pharmacology, University of Verona, Italy
(2) Laboratory of Cell Metabolism and Regenerative Medicine, Department of Medical Biotechnology and Translational Medicine, University of Milan, Milan, Italy

*Corresponding author: Ilaria Decimo, PhD
Sect. of Pharmacology
Dept. of Diagnostics and Public Health
University of Verona
P.le Scuro 10, 37134 Verona, Italy
tel: +39 045 802 7509
fax +39 045 802 7452
e-mail: ilaria.decimo@univr.it

ABSTRACT

Neural precursors (NPs) present in the hippocampus can be modulated by several neurogenic stimuli including environmental enrichment (EE) and antidepressant treatment acting through BDNF-TrkB signaling. We have recently identified NPs in meninges, however menigneal niche response to pro-neurogenic stimuli has never been investigated. To this aim, we analyzed the effects of 4 weeks fluoxetine administration or 1 week EE treatment on NP distribution in mouse brain meninges. Following neurogenic stimuli, although we did not detect modification of meningeal cell number and proliferation, we observed, in meninges, an increased number of β3-Tubulin$^+$ immature neuronal cells. Lineage-tracing experiment confirmed that EE-induced β3-Tubulin$^+$ immature neuronal cells present in meninges originated from GLAST$^+$ radial glia cells. To investigate the molecular mechanism responsible for this response, we studied the BDNF-TrkB interaction. Treatment with ANA-12, a TrkB non-competitive inhibitor, abolished the EE-induced increase of β3-Tubulin$^+$ immature neuronal cells in meninges. Overall these data showed, for the first time, that the meningeal niche responded to neurogenic stimuli by increasing the immature neuronal population through TrkB-mediated signaling. A better understanding of the neurogenic stimuli effects on NPs in meninges may be useful to improve the effectiveness of depression and mood disorders treatments.

KEYWORDS

Neurogenesis, TrkB, BDNF, Meninges, ANA-12, Neural cell differentiation

 doi:10.20944/preprints202106.0327.v1

DATA AVAILABILITY STATEMENT

The data that support the findings of this study are available from the corresponding author upon request.

INTRODUCTION

Mammal adult neurogenesis can be modulated by several stimuli including antidepressant treatment and exposure to enriched environment (EE) [1].
Fluoxetine, a Selective-Serotonin Reuptake Inhibitor (SSRI) antidepressant [2, 3], as well as other antidepressants, has been shown to induce hippocampal neurogenesis [3-5]. Similarly, EE also increases hippocampal neurogenesis and its therapeutic effect has been used to ameliorate brain injury outcomes [6]. The molecular mechanisms responsible for the hippocampal neurogenic modulation by EE and fluoxetine have not been fully elucidated; however, a major role of the BDNF-TrkB signaling pathway has been described by several groups [7-10]. Besides the fluoxetine and EE effects on the hippocampal neurogenesis, little is known about their effects on other less studied brain NSC niches. [11].
Recently, a subset of meningeal-residing neural progenitors has been identified both during development and adulthood in different mammals, including humans [11-16]. Single-cell RNA sequencing (scRNAseq) analysis of meningeal cells identified a small fraction of cells with a signature corresponding to radial glia-like cells, expressing GLAST and a population with a neuroblast signature expressing β3-Tubulin [17]. These neural precursors can migrate from the meninges to the brain parenchyma and differentiate into functional cortical neurons or oligodendrocytes [17, 18]. Meningeal stem cell niche is composed by specific trophic extracellular matrix components called fractones and it is able to sense and respond to neurotrophic stimuli including FGF2, NGF, and EGF [19-21]. Noteworthly, NPs in meninges have been shown to react to CNS diseases, including spinal cord and brain injuries, amygdala lesion, stroke and progressive ataxia [13, 22]. Meninges may therefore represent a functional niche for neural progenitors, however, the response of NPs in meninges to neurogenic stimuli such as drugs (i.e., fluoxetine) [23] or EE tasks [24] has never been assessed. In this work we investigated the effects and the molecular mechanisms of menigneal niche response to pro-neurogenic stimuli including antidepressant treatment and EE exposure.
We found that fluoxetine and EE increased the number of neural progenitors in meninges. Lineage tracing experiment further confirmed that EE-induced NPs in meninges derived from radial glia GLAST$^+$ cells. Pharmacological inhibition of TrkB receptor following EE administration abolished both the hippocampal and meningeal increase of neural progenitors supporting the role of TrkB-BDNF signaling in hippocampal and meningeal response to neurogenic stimuli.

Preprints (www.preprints.org) | NOT PEER-REVIEWED | Posted: 11 June 2021 doi:10.20944/preprints202106.0327.v1

RESULTS

Neural precursor cells and immature neurons increase in mouse brain meninges following Fluoxetine administration

Hippocampal adult neurogenesis can be enhanced by external stimuli such as antidepressant treatment [4, 25, 26]. Fluoxetine is a SSRI antidepressant which has been shown to ameliorate anxiety/depression-related behavior and hippocampal neurogenesis [4] .

To investigate if pro-neurogenic stimuli were able to induce changes in meningeal niche, we exposed CD1 mice (4 weeks old) to chronic (4 weeks) administration of fluoxetine as described by others (**Fig. 1A**)[3, 4, 27].

We first confirmed the effectiveness of the fluoxetine treatment on animal behavior using an anxiety/Obsessive Compulsive Disorder (OCD)-evaluating behavioral test (the Marble Burying Test, MBT) [28, 29]. As shown in **Figure 1B-C**, following 4 weeks of drug administration, the percentage of marbles buried by treated animals is significantly lower when compared with controls (percentage of marbles buried over the total marble number, CTRL: 79,33% ± 5,573, n=10; FLUOX: 31,37% ± 7,854, n=17; p=0,0002). As expected, the antidepressant was able to reduce OCD-like behavior and, thus, it suggested that fluoxetine exerted its pharmacological effect. We further confirmed fluoxetine efficacy on hippocampal neurogenesis by analyzing the expression of the proliferation marker Ki67 and of the immature neuron marker doublecortin (DCX) in the DG (**Fig. 1D-G**). In line with previous observations, we found that the number of $Ki67^+$ cells and the extension of the DCX^+ expression area of the dentate gyrus (DG) were significantly higher in fluoxetine-treated mice compared to control mice (number of $Ki67^+$ cells per mm^2 of DG area, CTRL 0,007801 ± 0,004454, n=3; FLUOX: 0,02541 ± 0,003082, n=3; p=0,0313) (percentage of DCX^+ area over the total DG area, CTRL: 1,381% ± 0,1229, n=3; FLUOX: 2,403% ± 0,1472, n=3; p=0,0060). These data confirmed fluoxetine treatment effectiveness, supporting its known effect on both OCD-like behavior and hippocampal neuronal differentiation [3, 4, 27].

A similar approach was used to characterize the possible antidepressant-induced effects on meninges. We first analyzed mouse brain meningeal cell number and proliferation following 4 weeks of fluoxetine treatment. The meningeal nuclei number as well as the number of cells expressing the proliferation marker Ki67 didn't change following the treatment (**Fig. 1H-K**). NPs in meninges are characterized by features of radial glia-like cells expressing GLAST and of immature neurons expressing β3-Tubulin [13]. We found that both $GLAST^+$ neural precursors and $β3\text{-}Tubulin^+$ cells increased in the treated group compared to the control (**Fig.1L-O**) (number of $GLAST^+$ cells per 2 mm of cross-sectioned meninges: CTRL: 9,167 ± 0,9458, n=6; FLUOX: 13,17 ± 1,352, n=6; p=0,0358; number of $β3\text{-}Tubulin^+$ cells per 2 mm of cross-sectioned meninges: CTRL: 14,6 ± 1,72, n=5; FLUOX: 32,6 ± 3,736, n=5; p=0,0024). These data suggested that meningeal niche responded to fluoxetine increasing NPs number.

We further investigated the impact of the antidepressant treatment on the meningeal niche by analyzing the extracellular matrix components and the innate immune cell macrophages [5, 30]. The meningeal niche is endowed of fractones, small laminin-based structures able to capture growth factors and exerting a trophic role for neural stem cells niche [31]. We therefore, analyzed the distribution of the fractones by analysing $laminin^+$ puncta [12]. Importantly, the number of fractones was significantly higher in the fluoxetine-

Preprints (www.preprints.org) | NOT PEER-REVIEWED | Posted: 11 June 2021 doi:10.20944/preprints202106.0327.v1

treated group when compared to controls (**Fig.1P-Q**) (number of fractones per 2 mm of cross-sectioned meninges: CTRL: 59 ± 0,5774, n=3; FLUOX: 76,33 ± 2,186, n=3; p= 0,0016), suggesting that a trophic activation of the meningeal niche was induced in response to neurogenic stimuli. Finally, as immune cells were proven to have an effect on neurogenesis [32], we assessed the number of macrophages in meningeal niche following fluoxetine treatment. We observed a trend suggesting a possible increase of $CD68^+$ cells in fluoxetine treated mice, albeit the difference was not of statistical significance (**Fig.1R-S**).

Altogether these data indicated that meningeal niche reacted to fluoxetine treatment by increasing neural precursors, immature neurons and the trophic ECM fractones suggesting sensitivity of meningeal NPs to neurogenic stimuli. acting on the hippocampal niche.

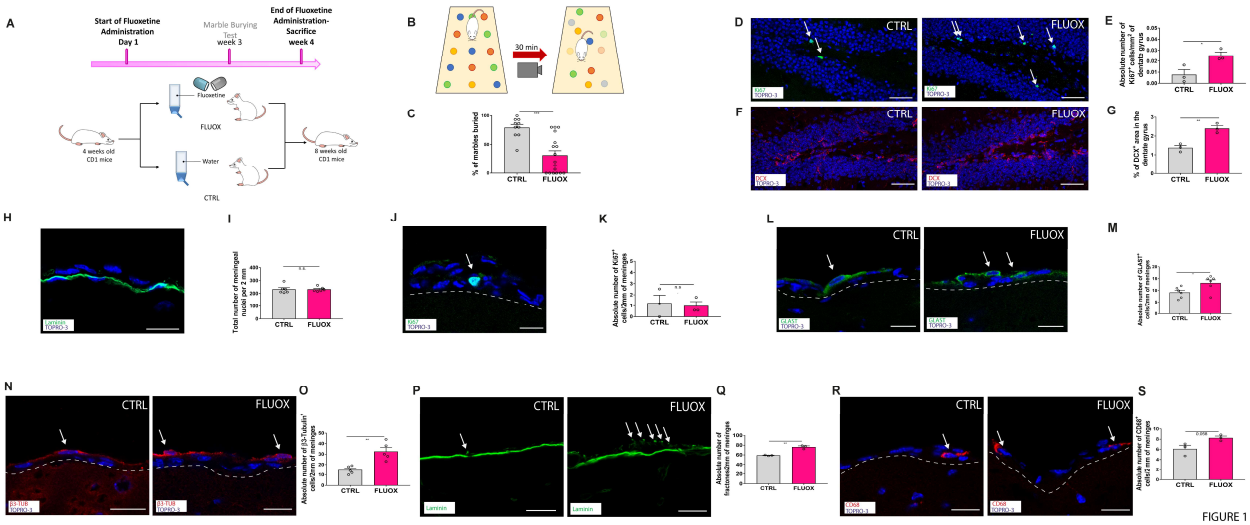

FIGURE 1 –MENINGEAL NICHE RESPONDS TO FLUOXETINE TREATMENT

(A) Schematic representation of the experimental design used for fluoxetine administration. **(B)** Schematic representation of behavioral testing for OCD-like behavior via Marble Burying Test (MBT). **(C)** Graph showing the percentage of marbles buried by treated (FLUOX) and non-treated (CTRL) animals. **(D, F)** Sagittal brain sections of CD1 mice, showing the presence of $Ki67^+$ cells (green) and DCX^+ cells (red) in hippocampal dentate gyri (DG) in FLUOX and CTRL animals. **(E, G)** Graphs showing the number of $Ki67^+$ cells per mm^2 of DG **(E)** and the percentage of DCX^+ area in the DG **(G)**. **(H)** Sagittal brain section of CD1 mice, showing brain meningeal nuclei and meningeal basal laminin and **(I)** graph showing the total number of meningeal nuclei. **(J)** Sagittal brain section of CD1 mice, showing brain meningeal $Ki67^+$ cells and **(K)** graph showing the $Ki67^+$ cells per 2 mm of meningeal tissue. **(L)** Sagittal brain sections of CD1 mice, showing brain meningeal $GLAST^+$ cells and **(M)** graph showing the $GLAST^+$ cells per 2 mm of meningeal tissue. **(N)** Sagittal brain sections of CD1 mice, showing brain meningeal β3-$Tubulin^+$ cells and **(O)** graph showing the β3-$Tubulin^+$ cells per 2 mm of meningeal tissue. **(P)** Sagittal brain sections of CD1 mice, showing brain meningeal fractones and **(Q)** graph showing the absolute number of meningeal fractones per 2 mm of meningeal tissue and. **(R)** Sagittal brain sections of CD1 mice, showing brain meningeal $CD68^+$ cells and **(S)** graph showing the $CD68^+$ cells per 2 mm of meningeal tissue. Data are presented as mean ± SEM; n.s. = not statistically significant, * = p value ≤ 0.05, ** = p value ≤ 0.01, *** = p value ≤ 0.001. In pictures **D, F, H, J, L, N, P, R** Ki67, GLAST and Laminin are shown in green, DCX, β3-Tubulin and CD68 in red while nuclei are in

Preprints (www.preprints.org) | NOT PEER-REVIEWED | Posted: 11 June 2021 doi:10.20944/preprints202106.0327.v1

blue (TOPRO-3 nuclear staining). Pictures **H, J, L, N, P, R** are single plane confocal images. Pictures **D** and **F** are maximum intensity projections of z-stack confocal images. Scale bars represent 200 µm **(D, F)** and 20 µm **(H, J, L, N, P, R)**.

Neural precursor cells and immature neurons change their representation in mouse brain meninges during EE

EE is a pro-neurogenic stimulus known to have an antidepressant-like effect on hippocampal neurogenesis. In order to assess the effectiveness of the EE treatment on the meningeal niche, we exposed to EE CD1 mice for 7 days and then analyzed mouse brain by immunofluorescence and confocal analysis (**Fig.2A**). To validate EE treatment, we first assessed its impact on hippocampal neurogenesis by analyzing the number of cells expressing of the proliferation marker Ki67 and the extension of the DCX-labelled area in the DG (**Fig.2B-E**). The number of $Ki67^+$ cells and the DCX^+ area in DG of treated mice was significantly higher compared to control mice (number of $Ki67^+$ cells per mm^2 of DG area: CTRL: 0,02625 ± 0,005611, n=3; EE: 0,09301 ± 0,01854, n=3; p=0,0261; percentage of DCX^+ area over DG total area: CTRL:1,664% ± 0,3338, n=3; EE: 3,061% ± 0,2613, n=3; p=0,0300). In line with the literature data, these results confirmed that EE increased hippocampal neurogenesis [7, 33, 34].

To investigate if EE affected meningeal niche, we analyzed the number of cell nuclei and the expression of cell proliferation marker Ki67 in 2 mm of cross-sectioned brain meninges (**Fig.2F-G**). We didn't observe differences in both total cell number and proliferation index in meninges of control and EE treated group. Then, we analyzed in meninges the distribution of radial glia-like cells expressing GLAST and of immature neurons expressing β3-Tubulin (**Fig.2H-K**). We found a significant increase of $GLAST^+$ and β3-$Tubulin^+$ cells in treated mice as compared to the control group (number of $GLAST^+$ cells per 2 mm of cross-sectioned meninges: CTRL: 8 ± 0,5774, n=3; EE: 12,17 ± 0,6009, n=3; p=0,0075; number of β3-$Tubulin^+$ cells per 2 mm of cross-sectioned meninges: CTRL: 11 ± 1,528, n=3; EE: 20,67 ± 1,667, n=3; p=0,0129). In line with the results obtained by fluoxetine administration, these data indicated that meningeal niche responded to the EE neurogenic stimulus by increasing NP cell number.

We then focused our analysis on the evaluation of the meningeal trophic and immune state in response to this pro-neurogenic stimulus via quantification of the ECM component fractones and macrophages (**Fig.2L-O**). Similarly to fluoxetine experiments, we found a statistically significant increase in the meningeal fractones and in $CD68^+$ cells after exposure to EE (number of fractones per 2 mm of cross-sectioned meninges: CTRL: 47 ± 11,58, n=4; EE: 94,25 ± 10,17, n=4; p=0,0220; number of $CD68^+$ cells per 2 mm of cross-sectioned meninges: CTRL: 4,7 ± 0,05774, n=3; EE: 6,687 ± 0,5203, n=3; p= 0,0192).

These data indicated that neural precursor cells, immature neurons, fractones and macrophages significantly increased in brain meninges after EE exposure, further supporting the responsiveness of meningeal niche to pro-neurogenic stimuli.

Preprints (www.preprints.org) | NOT PEER-REVIEWED | Posted: 11 June 2021 doi:10.20944/preprints202106.0327.v1

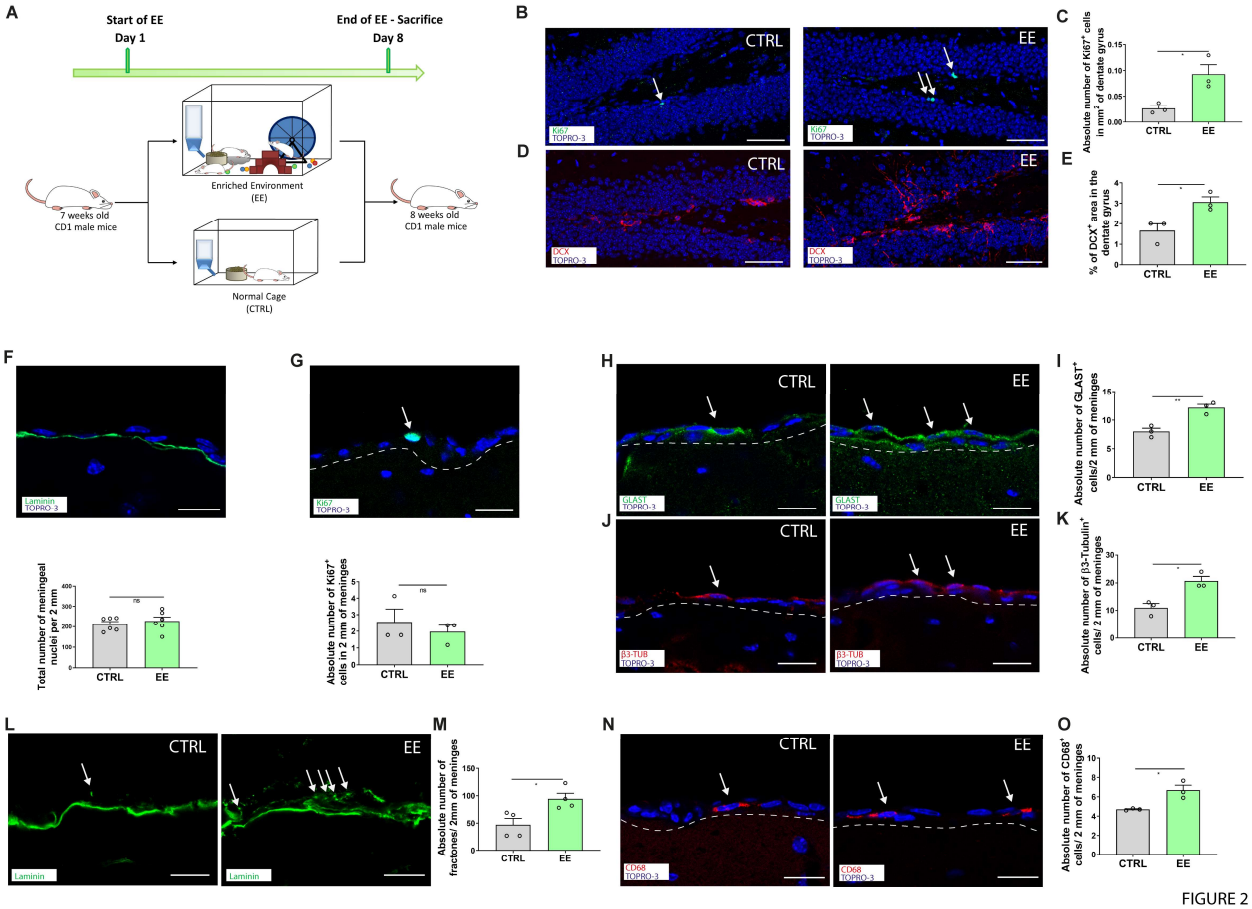

FIGURE 2

FIGURE 2 – MENINGEAL NICHE IS RESPONSIVE TO ENRICHED ENVIRONMENT STIMULUS

(A) Schematic representation of the experimental design used for Enriched Environment (EE) paradigm. **(B, D)** Sagittal brain sections of CD1 mice, showing the number of Ki67$^+$ cells (green) and the presence of DCX$^+$ cells (red) in hippocampal dentate gyri (DG) in control (CTRL) and in EE-exposed (EE) animals. **(C, E)** Graphs showing the number of Ki67$^+$ cells per mm^2 of DG **(C)** and the percentage of DCX$^+$ area in the DG **(E)**. **(F)** Graph showing the total number of meningeal nuclei and sagittal brain section of CD1 mice, showing brain meningeal nuclei and meningeal basal laminin. **(G)** Graph showing the Ki67$^+$ cells per 2 mm of meningeal tissue and sagittal brain section of CD1 mice, showing brain meningeal Ki67$^+$ cells. **(H)** Sagittal brain sections of CD1 mice, showing brain meningeal GLAST$^+$ cells and **(I)** graph showing the GLAST$^+$ cells per 2 mm of meningeal tissue. **(J)** Sagittal brain sections of CD1 mice, showing brain meningeal β3-Tubulin$^+$ cells and **(K)** graph showing the β3-Tubulin$^+$ cells per 2 mm of meningeal tissue. **(L)** Sagittal brain sections of CD1 mice, showing brain meningeal fractones and **(M)** graph showing the absolute number of meningeal fractones per 2 mm of meninges. **(N)** Sagittal brain sections of CD1 mice, showing brain meningeal CD68$^+$ cells and **(O)** graph showing the absolute number of CD68$^+$ cells per 2 mm of meningeal tissue. Data are presented as mean ± SEM; n.s. = not statistically significant, * = p value ≤ 0.05, ** = p value ≤ 0.01. In pictures **B, D, F, G, H, J, L, N** Ki67, GLAST and Laminin are shown in green, DCX, β3-Tubulin and CD68 in red while nuclei are in blue (TOPRO-3 nuclear staining). Pictures **F, G, H, J, L, N** are single plane confocal images. Pictures **B** and **D** are maximum intensity projections of z-stack confocal images. Scale bars represent 200 μm **(B, D)** and 20 μm **(F, G, H, J, L, N)**.

Preprints (www.preprints.org) | NOT PEER-REVIEWED | Posted: 11 June 2021 doi:10.20944/preprints202106.0327.v1

EE-induced NPs in meninges derive from GLAST$^+$ radial glia progenitors

To identify the lineage of the immature neurons which increased in meninges after the exposure to a pro-neurogenic stimulus, we took advantage of an inducible transgenic mouse model for radial-glial cells. GLAST-Cre^{ERT2} mice [35] intercrossed with the CAG-CAT-EGFP reporter line [36] (GLAST-GFP) allowed to label by GFP all the GLAST$^+$ cells and their progeny following tamoxifen administration. After three days of tamoxifen induction via oral gavage, we subjected the mice to two weeks of EE (**Fig.3A**) and then analysed the brain and meninges of control and treated mice [35].

At first, we confirmed the effectiveness of the EE protocol in GLAST-GFP mice by assessing the increase of DCX expression in the DG of treated mice (**Fig.3B, D**) (percentage of DCX$^+$ area over the total DG area, CTRL: 1,021 ± 0,1381, n=4; EE: 1,833 ± 0,319, n=3; p= 0,0485). In line with the results obtained in CD1 mice, we observed an increase of immature neurons in meninges as a response to EE exposure (**Fig.3 C, E)** (number of β3-Tubulin$^+$ cells per 2 mm of cross-sectioned meninges: CTRL: 11,33 ± 0,3333, n=3; EE: 18,3 ± 2,197, n=4; p= 0,0447).

We then analyzed the distribution and fate of GFP$^+$ GLAST-derived progenitors. As expected, we found GFP$^+$ cells in SVZ, DG and meninges both in EE-treated and control mice (**Fig.3F**) [35]. In order to assess the fate of the GFP$^+$ cells in meninges following EE exposure, we analyzed the expression of the β3-Tubulin in these cells (**Fig.3G-H**). We found the presence of a double positive GFP$^+$/ β3-Tubulin$^+$ cell population in EE treated mice meninges; on the contrary, double positive cells were absent in control mice, suggesting that immature neurons differentiated from GLAST derived cells (number of GFP$^+$/ β3-Tubulin$^+$ cells per 2 mm of cross-sectioned meninges: CTRL: 0 ± 0, n=3; EE: 1,478 ± 0,2629, n=8; p= 0,0088).

Altogether, these data indicate that increased β3-Tubulin$^+$ immature neurons in meninges following EE exposure originated from radial glia GLAST$^+$ cells.

Preprints (www.preprints.org) | NOT PEER-REVIEWED | Posted: 11 June 2021 doi:10.20944/preprints202106.0327.v1

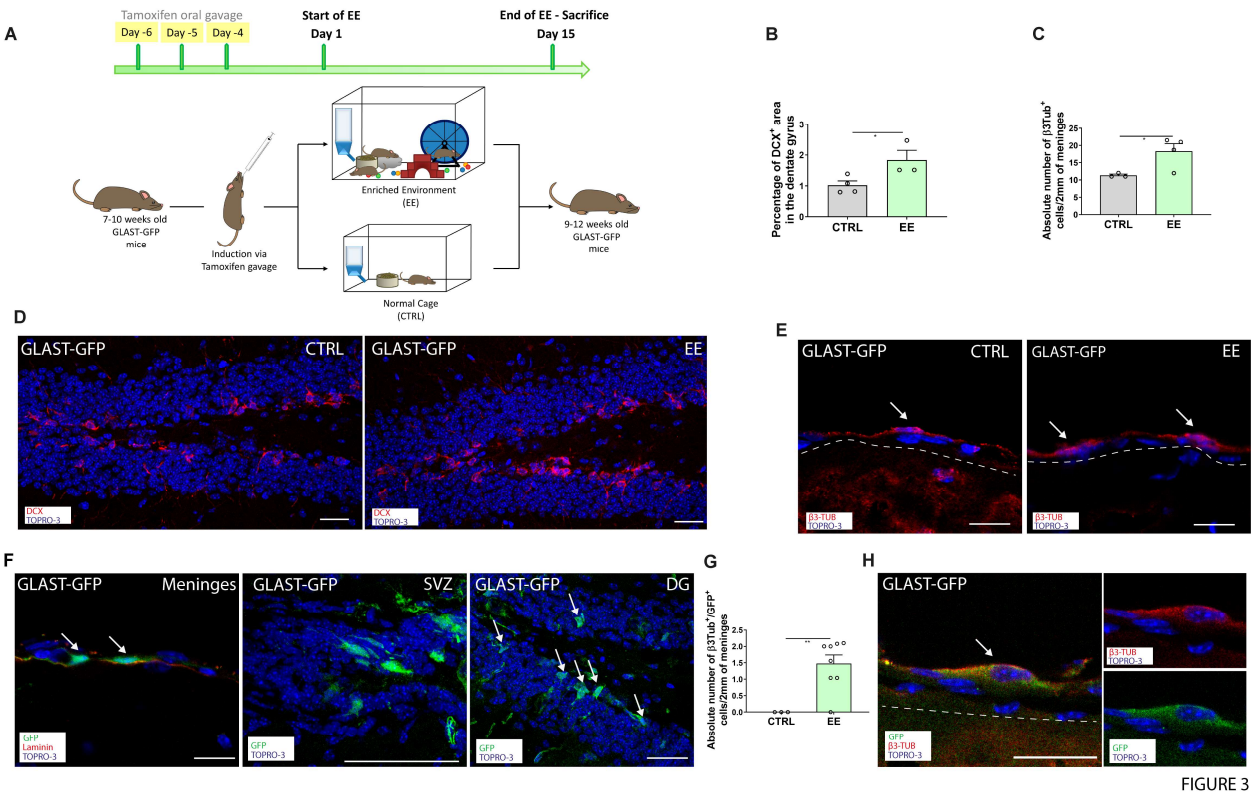

FIGURE 3

FIGURE 3 –LINEAGE TRACING CONFIRMS RADIAL GLIAL ORIGIN OF THE EE-INDUCED IMMATURE NEURONS

(A) Schematic representation of the experimental design. **(B)** Graph showing the percentage of DCX$^+$ area in the DG of EE and CTRL animals. **(D)** Sagittal brain sections of GLAST-GFP mice, showing the presence of DCX$^+$ cells (red) in hippocampal dentate gyri (DG) in CTRL and EE animals **(C)** Graph showing the β3-Tubulin$^+$ cells per 2 mm of meningeal tissue and **(E)** sagittal brain sections of GLAST-GFP mice, showing brain meningeal β3-Tubulin$^+$ cells. **(F)** Sagittal brain sections of GLAST-GFP mice, showing GFP$^+$ cells in brain meninges (MEN), in subventricular zone (SVZ) and DG. **(G)** Graph showing the GFP/β3-Tubulin$^+$ cells per 2 mm of meningeal tissue and **(H)** sagittal brain section of GLAST-GFP mice, showing brain meningeal GFP/β3-Tubulin$^+$ cells. Data are presented as mean ± SEM; * = p value ≤ 0.05, ** = p value ≤ 0.01. In **(D, E, F, H)** GFP is shown in green, DCX, laminin and β3-Tubulin in red while nuclei are in blue (TOPRO-3 nuclear staining). Pictures **E, F, H** are single plane confocal images. Pictures **D** are maximum intensity projections of z-stack confocal images. Scale bars represent 200 μm **(D)** and 20 μm **(E, F, H)**.

TrkB/BDNF signaling blockage abolishes Enriched Environment-mediated effects on meningeal neural precursors and immature neurons

It's known that fluoxetine and EE-mediated neurogenesis is carried out via molecular mediators including the BDNF/TrkB signaling pathway [3, 7]. TrkB, was identified as a gene expressed by the meningeal niche [17]. To investigate if this pathway was involved in the meningeal response to neurogenic stimuli, we first assessed the expression of TrkB in meningeal cells.

We found a significant increase of the TrkB$^+$ meningeal cell population following fluoxetine and EE administration (number of TrkB$^+$ cells per 2 mm of cross-sectioned meninges:

Preprints (www.preprints.org) | NOT PEER-REVIEWED | Posted: 11 June 2021 doi:10.20944/preprints202106.0327.v1

CTRL: 3 ± 1,472, n=4; FLUOX: 8,75 ± 0,4787, n=4; p=0,0099; number of TrkB$^+$ cells per 2 mm of cross-sectioned meninges: CTRL: 2,333 ± 0,8819, n=3; EE: 7,333 ± 0,8819, n=3; p=0,0160) (**Fig. 4A-D**). In addition, we identified a rare population of immature neurons co-expressing β3-Tubulin and the BDNF receptor TrkB. While this double positive population was extremely sporadic in the control animals, it was significantly present in both fluoxetine (number of β3-Tubulin$^+$/TrkB$^+$ cells per 2 mm of cross-sectioned meninges: CTRL: 1,8 ± 0,5831, n=5; FLUOX: 5,6 ± 1,327, n=5; p=0,0305) and EE (number of β3-Tubulin$^+$/TrkB$^+$ cells per 2 mm of cross-sectioned meninges: CTRL: 1 ± 0,5774, n=3; EE: 4,333 ± 0,8819, n=3; p=0,0341) treated groups (**Fig. 4E-H**). We further confirmed the increased expression of TrkB in GLAST-derived progenitors in meninges by using GLAST-GFP mice induced with tamoxifen for 3 days and subjected to EE for two weeks (number of GFP$^+$/TrkB$^+$ cells per 2 mm of cross-sectioned meninges: CTRL: 0,6667 ± 0,3333, n=3; EE: 3,488 ± 0,8236, n=5; p= 0,0460) (**Fig. 4I-J**).

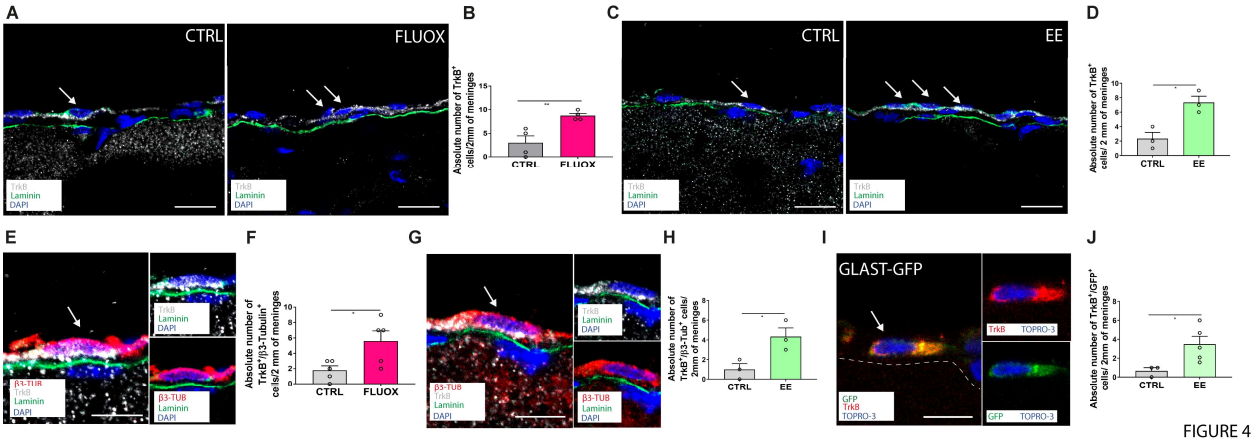

FIGURE 4 –MENINGEAL IMMATURE NEURONS EXPRESS THE NEUROTROPHIN RECEPTOR TRKB
(A) Sagittal brain sections of CD1 mice, showing brain meningeal TrkB$^+$ cells in Fluoxetine-treated (FLUOX) and control (CTRL) animals. **(B)** Graph showing the TrkB$^+$ cells per 2 mm of meningeal tissue. **(C)** Sagittal brain sections of CD1 mice, showing brain meningeal TrkB$^+$ cells in EE-exposed (EE) and control (CTRL) animals. **(D)** Graph showing the TrkB$^+$ cells per 2 mm of meningeal tissue. **(E)** Sagittal brain section of CD1 mice, showing brain meningeal β3-Tubulin$^+$/TrkB$^+$ cells. **(F)** Graph showing the β3-Tubulin$^+$ /TrkB$^+$ cells per 2 mm of meningeal tissue in FLUOX and CTRL animals. **(G)** Sagittal brain section of CD1 mice, showing brain meningeal β3-Tubulin$^+$/TrkB$^+$ cells. **(H)** Graph showing the β3-Tubulin$^+$ /TrkB$^+$ cells per 2 mm of meningeal tissue in EE and CTRL animals. **(I)** Sagittal brain section of GLAST-GFP mice, showing brain meningeal GFP$^+$/TrkB$^+$ cells**. (J)** Graph showing the GFP$^+$/TrkB$^+$ cells per 2 mm of meningeal tissue in EE and CTRL animals. In **(A, C, E, G, I)** laminin and GFP are shown in green, TrkB is shown in white, β3-Tubulin in red while nuclei are in blue (TOPRO-3 or DAPI nuclear staining). In **(I)** TrkB is shown in red. All pictures are single plane confocal images. Scale bars represent 20 μm **(A, C)** and 10 μm **(E, G, I)**.

TrkB receptor activation is inhibited by ANA-12, a non-competitive inhibitor. In order to provide evidences that meningeal response was directly regulated by the activation of the neurotrophic receptor TrkB, we administrated ANA-12 to CD1 mice 3 days prior and at the 3rd day during EE exposure [37] (**Fig. 5A**).

Preprints (www.preprints.org) | NOT PEER-REVIEWED | Posted: 11 June 2021 doi:10.20944/preprints202106.0327.v1

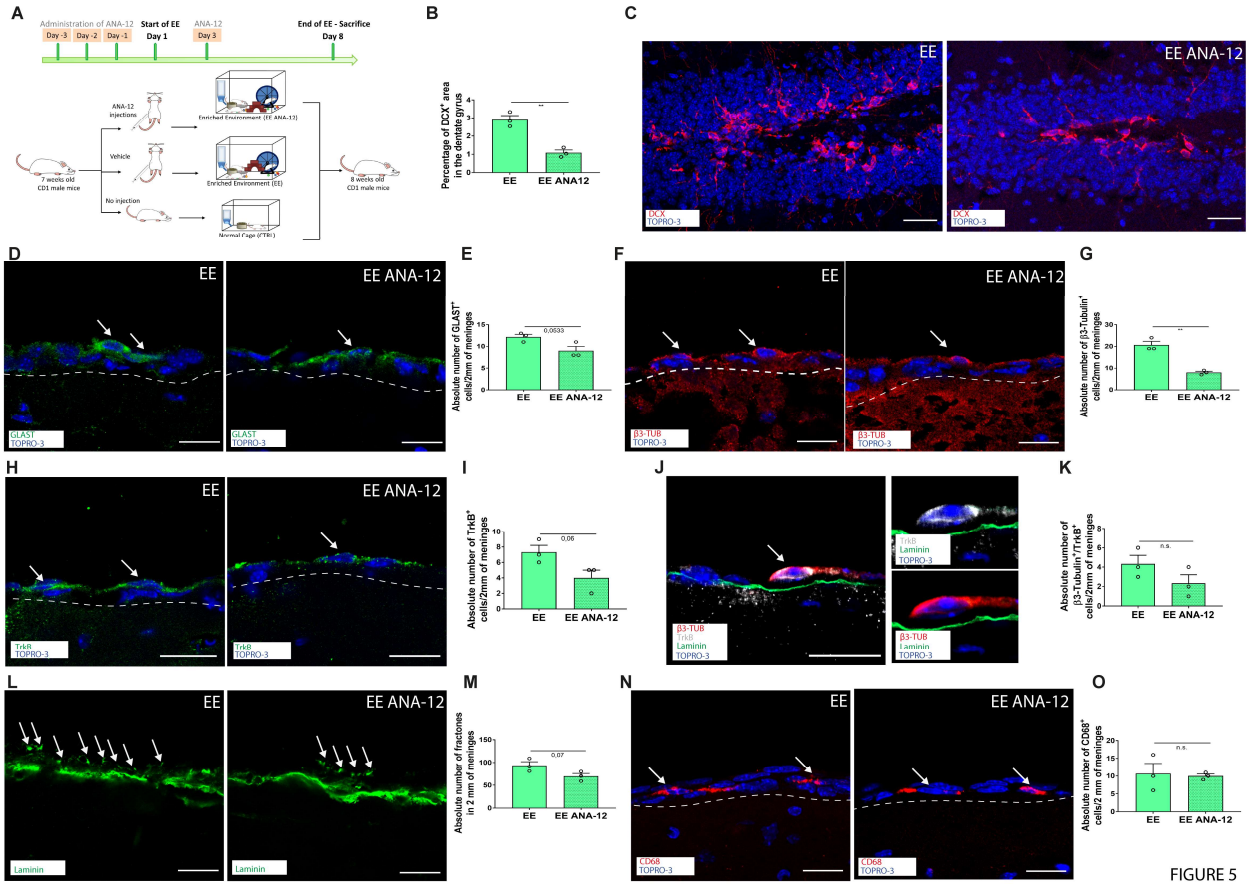

FIGURE 5

FIGURE 5 –TRKB/BDNF SIGNALING IS REQUIRED FOR MENINGEAL RESPONSE TO EE STIMULUS

(A) Schematic representation of the experimental design used to test BDNF/TrkB dependency of meningeal response to EE. **(B)** Graph showing the percentage of DCX$^+$ area in the DG of animals EE ANA-12 and EE. **(C)** Sagittal brain sections of CD1 mice, showing the presence of DCX$^+$ cells (red) in hippocampal dentate gyri (DG) in animals exposed to EE and injected with TrkB inhibitor ANA-12 (EE ANA-12) or vehicle (EE). **(D)** Sagittal brain sections of CD1 mice, showing brain meningeal GLAST$^+$ cells and **(E)** graph showing the GLAST$^+$ cells per 2 mm of meningeal tissue. **(F)** Sagittal brain sections of CD1 mice, showing brain meningeal β3-Tubulin$^+$ cells and **(G)** graph showing the β3-Tubulin$^+$ cells per 2 mm of meningeal tissue. **(H)** Sagittal brain sections of CD1 mice, showing brain meningeal TrkB$^+$ cells and **(I)** graph showing the TrkB$^+$ cells per 2 mm of meningeal tissue. **(J)** Sagittal brain section of CD1 mice, showing brain meningeal TrkB/β3-Tubulin$^+$ cells and **(K)** graph showing the TrkB/β3-Tubulin$^+$ cells per 2 mm of meningeal tissue. **(L)** Sagittal brain sections of CD1 mice, showing brain meningeal fractones and **(M)** graph showing the absolute number of meningeal fractones per 2 mm of meninges. **(N)** Sagittal brain sections of CD1 mice, showing brain meningeal CD68$^+$ cells and and **(O)** Graph showing the absolute number of CD68$^+$ cells per 2 mm of meningeal tissue. Data are presented as mean ± SEM; n.s. = not statistically significant, * = p value ≤ 0.05, ** = p value ≤ 0.01. In **(C, D, F, H, J, L, N)** GLAST, TrkB and laminin are shown in green, DCX, β3-Tubulin and CD68 in red while nuclei are in blue (TOPRO-3 or DAPI nuclear staining). In **(J)** TrkB is in white. Pictures **D, F, H, J, L, N** are single plane confocal images. Pictures **C** are maximum intensity projections of z-stack confocal images. Scale bars represent 200 μm **(C)** and 20 μm **(D, F, H, J, L, N)**.

At first, we assessed if the inhibitor was able to ablate the canonical effects caused by EE on the hippocampal neurogenesis. As expected, ANA-12 ablated the EE neurogenic

Preprints (www.preprints.org) | NOT PEER-REVIEWED | Posted: 11 June 2021 doi:10.20944/preprints202106.0327.v1

effects on DG (percentage of DCX$^+$ area over total DG area: EE: 2,899 ± 0,2315, n=3; EE+ANA-12: 1,085 ± 0,1515, n=3; p=0,0028) **(Fig. 5B-C)**. These results validated the effect of ANA-12 on the hippocampal neurogenesis.

We then verified whether also the changes observed in meninges after EE exposure could be reversed by blocking the TrkB/BDNF signaling. We found that GLAST$^+$ progenitors decreased slightly in the EE-treated group after the co-administration of ANA-12, although this difference was not statistically relevant (number of GLAST$^+$ cells per 2 mm of cross-sectioned meninges: EE: 12,17 ± 0,6009, n=3; EE ANA-12: 9 ± 1, n=3; p=0,0533) (**Fig. 5D-E**). We also observed that the EE-induced increase in the β3-Tubulin$^+$ population was completely ablated when the TrkB inhibitor was administered (**Fig. 5F-G**) (number of β3-Tubulin$^+$ cells per 2 mm of cross-sectioned meninges, EE: 20,67 ± 1,667, n=3 ; EE ANA-12: 8 ± 0,5774, n=3; p= 0,0020).

A non-statistically significant reduction in the number of TrkB$^+$ cells in meninges was also observed following ANA-12 treatment (number of TrkB$^+$ cells per 2 mm of cross-sectioned meninges: EE: 7,333 ± 0,8819, n=3; EE ANA-12: 4 ± 1, n=3; p= 0,0668) (**Fig. 5 H-I**). A similar non-statistically-significant reduction in the number of immature neurons expressing TrkB occurred when administering the inhibitor to the EE-treated animals (**Fig. 5 J-K**) (number of β3-Tubulin$^+$/TrkB$^+$ cells per 2 mm of cross-sectioned meninges: EE: 4,333 ± 0,8819, n=3; EE ANA-12: 2,333 ± 0,8819, n=3; p= 0,1841).

These data suggested that the administration of ANA-12 may interfere with capacity of the immature neurons to react to neurogenic stimuli and to express the BDNF receptor.

We then, assessed the effect of ANA-12 inhibition on the trophic and immune state of the meningeal niche. Interestingly, the increase in fractones in meninges after EE exposure was partially reduced by ANA-12 administration, suggesting its partial dependence on TrkB/BDNF signaling (number of fractones per 2 mm of cross-sectioned meninges: EE: 93,67 ± 8,192, n=3; EE ANA-12: 69,67 ± 6,064, n=3; p= 0,0781), while we didn't identify any reduction trend in the number of CD68$^+$ cells in meninges (**Fig. 5 L-O**).

Overall, the data suggest that meningeal niche response to neurogenic stimuli was, at least in part, mediated by the neurotrophic receptor TrkB.

DISCUSSION

In this study, we described, for the first time, the meningeal niche response to neurogenic stimuli. Following fluoxetine and EE administration, meninges increased the number of immature neurons. In addition, administration of the TrkB blocker ANA-12 [38] inhibited this response, suggesting that the effects of neurogenic stimuli on the meningeal niche is at least in part mediated by BDNF receptor signaling.

Hippocampal neurogenesis has been extensively investigated with pro-neurogenic paradigms like EE and antidepressant treatments. However, the effect of neurogenic stimuli on novel less-known NSC niches, like the meningeal one, is still unexplored [4, 7, 33]. We first verified the effectiveness of the pro-neurogenic stimuli active on hippocampal neurogenesis, then we investigated meningeal niche responses. Strikingly, in both fluoxetine and EE administration, we observed an increase in GLAST$^+$ NPs and in β3-Tubulin$^+$ immature neurons, without cellular proliferation. The meningeal response to neurogenic stimuli partially differs from the hippocampal one [4, 26, 33, 39, 40], as there's no apparent increase in cellular proliferation. However, the overall increase of immature neurons was observed in both meninges and hippocampus.

Meningeal niche was already shown to be able to sense and respond to different type of stimuli both in physiological and pathological conditions. Administration of FGF-2 and NGF in meninges induced hyperplastic changes within the meninges of the rat and monkey [20, 21]. Injuries, including spinal cord injury (SCI) [22], progressive ataxia [41] and brain stroke [42] were able to increase the number of meningeal-derived doublecortin (DCX) positive immature neurons.

Aside from effects on immature neurons and neural progenitors, the pro-neurogenic stimuli used in our study were also able to remodel in a significant way the extracellular matrix. In both neurogenic paradigms, we observed an increase in the fractones, specialized ECM components of the neurogenic niche able to retain trophic factors [43] suggesting an overall remodeling of the meningeal niche. As the presence/increase of fractones in a NSC niche has been associated with neurogenesis, this further corroborates the hypothesis that the responsiveness of meninges to EE and fluoxetine treatment is a form of neurogenesis, albeit different from the hippocampal one [31].

While the mechanisms underlying the pro-neurogenic effects of antidepressants and environmental enrichment have been not entirely clarified, the pivotal role played by BDNF in these contexts has been shown [4, 7]. We examined BDNF role using ANA-12, a small molecule acting as a TrkB non-competitive inhibitor [38]. We observed that the effects on β3-Tubulin and TrkB expression induced by EE were partially reverted by ANA-12 administration. The number of $CD68^+$ cells was not altered by the TrkB inhibitor, while a reduction trend in the number of meningeal fractones was observed suggesting that macrophage activity to generate ECM was partially reduced [43].

To identify the origin of the immature neurons emerging in meninges after the exposure to the neurogenic stimuli, we took advantage of a transgenic model used for radial-glia (RG) cells tracing [35, 36]. We observed that GFP^+ radial glia derived neural precursors co-expressing TrkB and β3-Tubulin increased in meninges following EE administration suggesting the RG origin of the immature neurons. The RG origin of neurons present in the meningeal niche was already characterized in the healthy newborn mouse [17]; here we showed for the first time their presence in the adult mouse brain. The increase in the number of immature neurons observed in meninges after the pro-neurogenic stimulus may be due to differentiation of RG endogenous cells already present in meninges or to neural precursors migrating from brain neurogenic niche to the meninges.

While the findings regarding the generation of immature neurons in brain meninges after exposure to neurogenic stimuli are completely novel, one question, out of many, remains to be answered: what is the function of these cells? In recent years, the presence of “stand-by” neuroblasts expressing markers of neural precursors (like nestin or GLAST) or of migrating cells (like DCX) while being in a quiescent state (no expression of Ki67, no BrdU incorporation) was described [11, 44-46]. Those quiescent cells were found in classical NSC niches, like the subgranular [47, 48] and the subventricular zone [49], but also in newly described niches like the cortex, the striatum and the meninges themselves [11, 17, 47, 50-52]. The role covered by those stand-by neuroblasts is still object of speculation and hypothesis, as little is known about their function in the adult brain. Our study showed that, at least in meninges, quiescent precursors are sensitive to pro-neurogenic stimuli. This opens the stage to further investigations that may help clarifying the function of immature neurons in the regeneration and/or repair processes occurring in adult brain.

Preprints (www.preprints.org) | NOT PEER-REVIEWED | Posted: 11 June 2021 doi:10.20944/preprints202106.0327.v1

MATERIAL AND METHODS

Animals

Animal housing and all experimental procedures were approved by the Istituto Superiore della Sanita` (I.S.S., National Institute of Health), Italy and the Animal Ethics Committee (C.I.R.S.A.L., Centro Interdipartimentale di Servizio alla Ricerca Sperimentale) of the University of Verona, Italy (authorization number: 237/2016-PR; date of approval: 3rd March 2016; protocol number: 56DC9.13). Wild-type (WT) CD1 mice and GLAST -GFP transgenic mice [35, 36] were used for all the experiments.

CD1 mice Fluoxetine administration

Four weeks old CD1 male and female mice (n=25) were treated via oral administration of fluoxetine (Fluoxetine Hydrochloride, LRAA9180, Sigma-Aldrich, St. Louis) for 4 consecutive weeks. The drug was dissolved into the water (0.16 mg/ml concentration) contained in the dispenser normally present in mice cages, and mice were able to access freely the water containing the drug. As fluoxetine is light-sensitive, a tinfoil sheet was used to cover the water dispenser, in order to avoid any kind of light-induced change on the drug. The drug-containing water was changed by the operator two times per week and the dispenser was weighted to evaluate the average water consumption for every animal. On the basis of this evaluation, on average, animals took 29 mg/kg/die of fluoxetine via parenteral administration. The control group consisted in equally aged CD1 male and female mice (n=15) which were administrated normal water.

CD1 mice exposure to Enriched Environment

Seven weeks old CD1 male mice (n=6) were housed together in a single rat cage for 1 week of time. A running wheel and nesting material were always present in the cage, while other toys (stairs, cardboard rolls and marbles) were added alternatively to the cage, in order to preserve novelty, according to what is shown in Table 1. Animals were sacrificed after 7 days of EE exposure. Control animals were equally aged CD1 male mice (n=5) housed singularly for 1 week of time. The cage was a normal mouse cage and no toys were introduced in the cages for the whole experiment. Animals were sacrificed 7 days after the start of the experiment.

TABLE 1 Scheme of the toys differentially used to perform the environmental enrichment on 7 weeks CD1 male mice. The X in the square states that the toy (raw) was present in the cage at that specific day (column). If a cell is empty, it means that the toy (row) wasn't present at that specific day (column).

TOYS	DAY 1	DAY 2	DAY 3	DAY 4	DAY 5	DAY 6	DAY 7
Running wheel	X	X	X	X	X	X	X
Nesting material	X	X	X	X	X	X	X
Cardboard rolls		X			X		X
Marbles			X		X	X	
Stairs				X		X	X

Preprints (www.preprints.org) | NOT PEER-REVIEWED | Posted: 11 June 2021 doi:10.20944/preprints202106.0327.v1

CD1 mice exposure to EE and TrkB inhibitor ANA-12

Seven weeks old CD1 male mice (n=6) were injected intraperitoneally with 10 µl/g of TrkB inhibitor ANA-12 [38] dissolved in sunflower seed oil + 1% DMSO at a 0,1 mg/ml concentration three consecutive days before the start of the experiment and at the third day of the experiment. This administration protocol was adapted from Moy et al 2019 [37]. After the injections, mice were either subjected to EE (n=3) as described above (CD1 mice exposure to Enriched Environment). Control vehicle animals were injected with vehicles only at the same time points as the ANA-12 treated ones, and then they were subjected to EE treatment for the same period of time.

GLAST-GFP exposure to EE

GLAST-Cre^{ERT2} mice [35] intercrossed with the CAG-CAT-EGFP reporter line [36] (GLAST-GFP) that allow to label by GFP all the GLAST^{+} cells and their progeny following tamoxifen administration, creating the GLAST-GFP strain. Seven to ten weeks old GLAST-GFP mice were induced using 3 daily Tamoxifen (T5648-1G, Sigma-Aldrich, St. Louis) gavage before the start of the EE protocol. Tamoxifen was dissolved into sunflower seed oil at a 30mg/ml concentration and the mice received 3.5mg of Tamoxifen for 35g of bodyweight. Animals were then left 2 days alone to recover from the handling and then were either subjected to EE (n=3) or control treatment (n=4) as previously described. Due to the mouse strain the treatment was prolonged to 2 weeks.

Marble Test Administration

Behavioral marble test was administrated at the end of the 3rd week of fluoxetine treatment. Animals were individually placed into a new cage containing 15 equally spaced marbles placed over approximately 5 cm of saw dust, and their behaviour was video-recorded for 30 minutes. The number of buried marbles (criterium of at least ¾ of its surface under the saw dust) was blindly assessed.

Tissue Preparation and Immunofluorescence

All animals were anesthetized by intraperitoneal injection of Zoletil (50 mg/kg) and Xylazine (7 mg/kg). Once the pedal reflex was lost, animals were sacrificed by intracardial perfusion of PBS with 4% paraformaldehyde (PFA)/4% sucrose (pH 7.4) solution. Brains were extracted, fixed in 4% PFA solution and transferred into 10% and subsequently 30% sucrose solution. By cryostat cutting, 35 µm thick medio lateral sagittal brain sections were obtained and processed by immunofluorescence as previously described [53]. Immunostaining on cryosections was performed after 30 minutes incubation in blocking solution (PBS 1X with 0.25% Triton X-100, 2% BSA). If required by the specific antibody combination, mouse serum (1:100) was added during incubation in blocking solution. Sections were then incubated with primary antibodies in blocking solution overnight at 4°C. After rinsing 6 times for 5 minutes in blocking solution, appropriate secondary antibodies were applied for 4 hours at room temperature. After final washing steps in blocking solution and then in PBS, nuclear staining with 4',6- Diamidino-2-Phenylindole Dihydrochloride (DAPI, Molecular Probes-Thermo Fisher Scientific) or TO- PRO™-3

Iodide (TO-PRO-3, Molecular Probes-Thermo Fisher Scientific) was performed and slides were mounted using 1,4-Diazabicyclo[2.2.2]octane (DABCO,Sigma-Aldrich). Staining for the nuclear marker of proliferation Ki67 required a different blocking solution (PBS 1X with 0.5% Triton X-100, 2% BSA).

For immunofluorescence using two rabbit antibodies, one conjugated and one non-conjugated, the following protocol was developed.
Cryosectioned sagittal sections were obtained as previously described. Immunostaining was performed after a 30 minutes incubation in blocking solution (PBS 1X with 0.25% Triton X-100, 2% BSA). Sections were then incubated with the non-conjugated rabbit primary antibody in blocking solution overnight at 4°C. After rinsing 6 times for 5 minutes in blocking solution, the appropriate secondary antibody was applied for 4 hours at room temperature. Following additional rinsing in blocking solution 6 times for 5 minutes, the GFP-conjugated antibody was added to the sections, which were incubated overnight at 4°C. Final washing steps, nuclear staining and mounting procedure were performed as previously described.

Antibodies

The following primary antibodies were used: anti-GLAST (anti-EAAT1; rabbit, 1:200, Abcam, AB416), anti-DCX (goat, 1:200, Santa Cruz, SC-8066), anti-DCX (rabbit, 1:400, Cell Signaling, 4604S), anti-β3 tubulin (mouse, 1:400, Promega, G7121), anti-laminin (rabbit, 1:400, Sigma-Aldrich, L9393), anti-laminin-Alexa Fluox 488 (1:500, Invitrogen, PA5-22901), anti-CD68 (rat, 1:200, Invitrogen, 14-0681-82), anti-TrkB (anti-tyrosin kinase receptor B, 1:200, rabbit, Santa Cruz, SC-12), anti-Ki67 (rabbit, 1:200, Abcam, AB16667), anti-GFP-Alexa Fluor 488 (rabbit, 1:500, Invitrogen, A21311),
The following secondary antibodies were used: donkey anti-rabbit Alexa Fluor 488 (1:500, Molecular Probes-Thermo Fisher Scientific), donkey anti-rabbit Alexa Fluox 647 (1:500, Molecular Probes-Thermo Fisher Scientific), donkey anti-goat Alexa Fluor 546 (1:500, Life Technologies-Thermo Fisher Scientific), goat anti-mouse CY3 (1:500, Jackson ImmunoResearch). For nuclear staining, TO-PRO™-3 (1:3000, Molecular Probes-Thermo Fisher Scientific) and DAPI (1:2000, Molecular Probes-Thermo Fisher Scientific) were used.

Quantitative Analysis

Quantification of different marker and nuclei was done by counting positive cells above the basal lamina (identified by laminin reactivity) in at least 18 sections for each experimental group (n ≥ 3 animals analyzed). For analysis on post hoc tissues, imaging of the immunostained slices was performed using an Eclipse Ti Nikon microscope (Nikon, Tokyo, Japan) and a Zeiss L710 confocal microscope (Carl Zeiss, Munich, Germany). Acquisition parameter settings (pinhole, gain, offset, laser intensity) were kept fixed for each channel in different sessions of observation at the fluorescence and confocal microscope.

Statistics

Data are expressed as mean ± SEM. Statistical differences were calculated by Student's t-test using GraphPadPrism (GraphPad Inc., La Jolla, CA). $p \leq 0.05$ was considered statistically significant.

ACKNOWLEDGMENTS

We acknowledge the CIRSAL (Centro Interdipartimentale di Servizi per la Ricerca che utilizza Animali da Laboratorio) for the help in the management of the animals needed for the experimental procedures. We thank Marzia Di Chio for her helpful technical assistance, Alberto Poli, Giulia Lucianer and Nicola Piazza for their help with immunofluorescence analysis. We acknowledge Prof. M. Goetz for kindly providing Glast-Cre ERT2 mice.

AUTHOR CONTRIBUTIONS

SZ performed experiments, analyzed and interpreted data, wrote the manuscript, final approval of manuscript; AC performed experiments, analyzed and interpreted data, wrote the manuscript, final approval of manuscript; AP collaborated for conceptualization and experiments on fluoxetine treatment; AA and FB contributed in confocal acquisition; GFF, CC, FB and ID reviewed the manuscript, final approval of manuscript and provided funding; FB and ID conceptualized the study; ID supervised the study.

CONFLICTS OF INTEREST

The authors declare that the research was conducted in the absence of any commercial or financial relationships that could be construed as a potential conflict of interest.

REFERENCES

1. Lu, J.; Manaenko, A.; Hu, Q., Targeting Adult Neurogenesis for Poststroke Therapy. *Stem Cells Int* **2017,** 2017, 5868632.
2. Ferguson, J. M., Mechanism of Action of Antidepressant Medications. *Primary Care Companion J Clin Psychiatry* **2001,** 3, (1), 22-27.
3. Samuels, B. A.; Hen, R., Neurogenesis and affective disorders. *Eur J Neurosci* **2011,** 33, (6), 1152-9.
4. David, D. J.; Samuels, B. A.; Rainer, Q.; Wang, J. W.; Marsteller, D.; Mendez, I.; Drew, M.; Craig, D. A.; Guiard, B. P.; Guilloux, J. P.; Artymyshyn, R. P.; Gardier, A. M.; Gerald, C.; Antonijevic, I. A.; Leonardo, E. D.; Hen, R., Neurogenesis-dependent and -independent effects of fluoxetine in an animal model of anxiety/depression. *Neuron* **2009,** 62, (4), 479-93.
5. Duman, R. S.; Monteggia, L. M., A neurotrophic model for stress-related mood disorders. *Biol Psychiatry* **2006,** 59, (12), 1116-27.
6. Forbes, T. A.; Goldstein, E. Z.; Dupree, J. L.; Jablonska, B.; Scafidi, J.; Adams, K. L.; Imamura, Y.; Hashimoto-Torii, K.; Gallo, V., Environmental enrichment ameliorates perinatal brain injury and promotes functional white matter recovery. *Nat Commun* **2020,** 11, (1), 964.
7. Eisinger, B. E.; Zhao, X., Identifying molecular mediators of environmentally enhanced neurogenesis. *Cell Tissue Res* **2018,** 371, (1), 7-21.
8. Bjorkholm, C.; Monteggia, L. M., BDNF - a key transducer of antidepressant effects. *Neuropharmacology* **2016,** 102, 72-9.

9. Kozisek, M. E.; Middlemas, D.; Bylund, D. B., Brain-derived neurotrophic factor and its receptor tropomyosin-related kinase B in the mechanism of action of antidepressant therapies. *Pharmacol Ther* **2008,** 117, (1), 30-51.
10. Casarotto, P. C.; Girych, M.; Fred, S. M.; Kovaleva, V.; Moliner, R.; Enkavi, G.; Biojone, C.; Cannarozzo, C.; Sahu, M. P.; Kaurinkoski, K.; Brunello, C. A.; Steinzeig, A.; Winkel, F.; Patil, S.; Vestring, S.; Serchov, T.; Diniz, C.; Laukkanen, L.; Cardon, I.; Antila, H.; Rog, T.; Piepponen, T. P.; Bramham, C. R.; Normann, C.; Lauri, S. E.; Saarma, M.; Vattulainen, I.; Castren, E., Antidepressant drugs act by directly binding to TRKB neurotrophin receptors. *Cell* **2021,** 184, (5), 1299-1313 e19.
11. Pino, A.; Fumagalli, G.; Bifari, F.; Decimo, I., New neurons in adult brain: distribution, molecular mechanisms and therapies. *Biochem Pharmacol* **2017,** 141, 4-22.
12. Bifari, F.; Berton, V.; Pino, A.; Kusalo, M.; Malpeli, G.; Di Chio, M.; Bersan, E.; Amato, E.; Scarpa, A.; Krampera, M.; Fumagalli, G.; Decimo, I., Meninges harbor cells expressing neural precursor markers during development and adulthood. *Front Cell Neurosci* **2015,** 9, 383.
13. Decimo, I.; Dolci, S.; Panuccio, G.; Riva, M.; Fumagalli, G.; Bifari, F., Meninges: A Widespread Niche of Neural Progenitors for the Brain. *Neuroscientist* **2020**, 1073858420954826.
14. Dolci, S.; Pino, A.; Berton, V.; Gonzalez, P.; Braga, A.; Fumagalli, M.; Bonfanti, E.; Malpeli, G.; Pari, F.; Zorzin, S.; Amoroso, C.; Moscon, D.; Rodriguez, F. J.; Fumagalli, G.; Bifari, F.; Decimo, I., High Yield of Adult Oligodendrocyte Lineage Cells Obtained from Meningeal Biopsy. *Front Pharmacol* **2017,** 8, 703.
15. Bifari, F.; Decimo, I.; Chiamulera, C.; Bersan, E.; Malpeli, G.; Johansson, J.; Lisi, V.; Bonetti, B.; Fumagalli, G.; Pizzolo, G.; Krampera, M., Novel stem/progenitor cells with neuronal differentiation potential reside in the leptomeningeal niche. *J Cell Mol Med* **2009,** 13, (9B), 3195-208.
16. Bifari, F.; Dolci, S.; Bottani, E.; Pino, A.; Di Chio, M.; Zorzin, S.; Ragni, M.; Zamfir, R. G.; Brunetti, D.; Bardelli, D.; Delfino, P.; Cattaneo, M. G.; Bordo, R.; Tedesco, L.; Rossi, F.; Bossolasco, P.; Corbo, V.; Fumagalli, G.; Nisoli, E.; Valerio, A.; Decimo, I., Complete neural stem cell (NSC) neuronal differentiation requires a branched chain amino acids-induced persistent metabolic shift towards energy metabolism. *Pharmacol Res* **2020,** 158, 104863.
17. Bifari, F.; Decimo, I.; Pino, A.; Llorens-Bobadilla, E.; Zhao, S.; Lange, C.; Panuccio, G.; Boeckx, B.; Thienpont, B.; Vinckier, S.; Wyns, S.; Bouche, A.; Lambrechts, D.; Giugliano, M.; Dewerchin, M.; Martin-Villalba, A.; Carmeliet, P., Neurogenic Radial Glia-like Cells in Meninges Migrate and Differentiate into Functionally Integrated Neurons in the Neonatal Cortex. *Cell Stem Cell* **2017,** 20, (3), 360-373 e7.
18. Dang, T. C.; Ishii, Y.; Nguyen, V.; Yamamoto, S.; Hamashima, T.; Okuno, N.; Nguyen, Q. L.; Sang, Y.; Ohkawa, N.; Saitoh, Y.; Shehata, M.; Takakura, N.; Fujimori, T.; Inokuchi, K.; Mori, H.; Andrae, J.; Betsholtz, C.; Sasahara, M., Powerful Homeostatic Control of Oligodendroglial Lineage by PDGFRalpha in Adult Brain. *Cell Rep* **2019,** 27, (4), 1073-1089 e5.
19. Nakagomi, T.; Molnar, Z.; Nakano-Doi, A.; Taguchi, A.; Saino, O.; Kubo, S.; Clausen, M.; Yoshikawa, H.; Nakagomi, N.; Matsuyama, T., Ischemia-induced neural stem/progenitor cells in the pia mater following cortical infarction. *Stem Cells Dev* **2011,** 20, (12), 2037-51.
20. Day-Lollini, P. A.; Stewart, G. R.; Taylor, M. J.; Johnson, R. M.; Chellman, G. J., Hyperplastic Changes within the Leptomeninges of the Rat and Monkey in Response to Chronic Intracerebroventricular Infusion of Nerve Growth Factor. *Experimental Neurology* **1997,** 145.

21. Parr, A. M.; Tator, C. H.; Keating, A., Bone marrow-derived mesenchymal stromal cells for the repair of central nervous system injury. *Bone Marrow Transplant* **2007,** 40, (7), 609-19.
22. Decimo, I.; Bifari, F.; Rodriguez, F. J.; Malpeli, G.; Dolci, S.; Lavarini, V.; Pretto, S.; Vasquez, S.; Sciancalepore, M.; Montalbano, A.; Berton, V.; Krampera, M.; Fumagalli, G., Nestin- and doublecortin-positive cells reside in adult spinal cord meninges and participate in injury-induced parenchymal reaction. *Stem Cells* **2011,** 29, (12), 2062-76.
23. Zhou, Q. G.; Lee, D.; Ro, E. J.; Suh, H., Regional-specific effect of fluoxetine on rapidly dividing progenitors along the dorsoventral axis of the hippocampus. *Sci Rep* **2016,** 6, 35572.
24. Kempermann, G.; Kuhn, H. G.; Gage, F. H., More hippocampal neurons in adult mice living in an enriched environment. *Nature* **1997,** 386.
25. Micheli, L.; Ceccarelli, M.; D'Andrea, G.; Tirone, F., Depression and adult neurogenesis: Positive effects of the antidepressant fluoxetine and of physical exercise. *Brain Res Bull* **2018,** 143, 181-193.
26. Wang, J. W.; David, D. J.; Monckton, J. E.; Battaglia, F.; Hen, R., Chronic fluoxetine stimulates maturation and synaptic plasticity of adult-born hippocampal granule cells. *J Neurosci* **2008,** 28, (6), 1374-84.
27. Khodanovich, M.; Kisel, A.; Kudabaeva, M.; Chernysheva, G.; Smolyakova, V.; Krutenkova, E.; Wasserlauf, I.; Plotnikov, M.; Yarnykh, V., Effects of Fluoxetine on Hippocampal Neurogenesis and Neuroprotection in the Model of Global Cerebral Ischemia in Rats. *Int J Mol Sci* **2018,** 19, (1).
28. Kraeuter, A. K.; Guest, P. C.; Sarnyai, Z., Object Burying Test for Assessment of Obsessive Compulsive Behaviors in Mice. *Methods Mol Biol* **2019,** 1916, 81-85.
29. de Brouwer, G.; Fick, A.; Harvey, B. H.; Wolmarans, W., A critical inquiry into marble-burying as a preclinical screening paradigm of relevance for anxiety and obsessive-compulsive disorder: Mapping the way forward. *Cogn Affect Behav Neurosci* **2019,** 19, (1), 1-39.
30. Sen, S.; Duman, R.; Sanacora, G., Serum brain-derived neurotrophic factor, depression, and antidepressant medications: meta-analyses and implications. *Biol Psychiatry* **2008,** 64, (6), 527-32.
31. Mercier, F., Fractones: extracellular matrix niche controlling stem cell fate and growth factor activity in the brain in health and disease. *Cell Mol Life Sci* **2016,** 73, (24), 4661-4674.
32. Ziv, Y.; Ron, N.; Butovsky, O.; Landa, G.; Sudai, E.; Greenberg, N.; Cohen, H.; Kipnis, J.; Schwartz, M., Immune cells contribute to the maintenance of neurogenesis and spatial learning abilities in adulthood. *Nat Neurosci* **2006,** 9, (2), 268-75.
33. Kempermann, G., Environmental enrichment, new neurons and the neurobiology of individuality. *Nat Rev Neurosci* **2019,** 20, (4), 235-245.
34. Young, D.; Lawlor, P. A.; Leone, P.; J., D. M. D. M., Environmental enrichment inhibits spontaneous apoptosis, prevents seizures and is neuroprotective. *Nature Medicine* **1999,** 5, 448-453.
35. Mori, T.; Tanaka, K.; Buffo, A.; Wurst, W.; Kuhn, R.; Gotz, M., Inducible gene deletion in astroglia and radial glia--a valuable tool for functional and lineage analysis. *Glia* **2006,** 54, (1), 21-34.
36. Nakamura, T.; Colbert, M. C.; Robbins, J., Neural crest cells retain multipotential characteristics in the developing valves and label the cardiac conduction system. *Circ Res* **2006,** 98, (12), 1547-54.
37. Moy, J. K.; Szabo-Pardi, T.; Tillu, D. V.; Megat, S.; Pradhan, G.; Kume, M.; Asiedu, M. N.; Burton, M. D.; Dussor, G.; Price, T. J., Temporal and sex differences in the role of

BDNF/TrkB signaling in hyperalgesic priming in mice and rats. *Neurobiol Pain* **2019,** 5, 100024.
38. Cazorla, M.; Premont, J.; Mann, A.; Girard, N.; Kellendonk, C.; Rognan, D., Identification of a low-molecular weight TrkB antagonist with anxiolytic and antidepressant activity in mice. *J Clin Invest* **2011,** 121, (5), 1846-57.
39. Sohur, U. S.; Emsley, J. G.; Mitchell, B. D.; Macklis, J. D., Adult neurogenesis and cellular brain repair with neural progenitors, precursors and stem cells. *Philos Trans R Soc Lond B Biol Sci* **2006,** 361, (1473), 1477-97.
40. Ming, G. L.; Song, H., Adult neurogenesis in the mammalian brain: significant answers and significant questions. *Neuron* **2011,** 70, (4), 687-702.
41. Kumar, M.; Csaba, Z.; Peineau, S.; Srivastava, R.; Rasika, S.; Mani, S.; Gressens, P.; El Ghouzzi, V., Endogenous cerebellar neurogenesis in adult mice with progressive ataxia. *Ann Clin Transl Neurol* **2014,** 1, (12), 968-81.
42. Nakagomi, T.; Molnar, Z.; Taguchi, A.; Nakano-Doi, A.; Lu, S.; Kasahara, Y.; Nakagomi, N.; Matsuyama, T., Leptomeningeal-derived doublecortin-expressing cells in poststroke brain. *Stem Cells Dev* **2012,** 21, (13), 2350-4.
43. Kerever, A.; Schnack, J.; Vellinga, D.; Ichikawa, N.; Moon, C.; Arikawa-Hirasawa, E.; Efird, J. T.; Mercier, F., Novel extracellular matrix structures in the neural stem cell niche capture the neurogenic factor fibroblast growth factor 2 from the extracellular milieu. *Stem Cells* **2007,** 25, (9), 2146-57.
44. Benedetti, B.; Dannehl, D.; Konig, R.; Coviello, S.; Kreutzer, C.; Zaunmair, P.; Jakubecova, D.; Weiger, T. M.; Aigner, L.; Nacher, J.; Engelhardt, M.; Couillard-Despres, S., Functional Integration of Neuronal Precursors in the Adult Murine Piriform Cortex. *Cereb Cortex* **2020,** 30, (3), 1499-1515.
45. La Rosa, C.; Ghibaudi, M.; Bonfanti, L., Newly Generated and Non-Newly Generated "Immature" Neurons in the Mammalian Brain: A Possible Reservoir of Young Cells to Prevent Brain Aging and Disease? *J Clin Med* **2019,** 8, (5).
46. La Rosa, C.; Cavallo, F.; Pecora, A.; Chincarini, M.; Ala, U.; Faulkes, C. G.; Nacher, J.; Cozzi, B.; Sherwood, C. C.; Amrein, I.; Bonfanti, L., Phylogenetic variation in cortical layer II immature neuron reservoir of mammals. *Elife* **2020,** 9.
47. Fuentealba, L. C.; Rompani, S. B.; Parraguez, J. I.; Obernier, K.; Romero, R.; Cepko, C. L.; Alvarez-Buylla, A., Embryonic Origin of Postnatal Neural Stem Cells. *Cell* **2015,** 161, (7), 1644-55.
48. Jhaveri, D. J.; O'Keeffe, I.; Robinson, G. J.; Zhao, Q. Y.; Zhang, Z. H.; Nink, V.; Narayanan, R. K.; Osborne, G. W.; Wray, N. R.; Bartlett, P. F., Purification of neural precursor cells reveals the presence of distinct, stimulus-specific subpopulations of quiescent precursors in the adult mouse hippocampus. *J Neurosci* **2015,** 35, (21), 8132-44.
49. Ottone, C.; Krusche, B.; Whitby, A.; Clements, M.; Quadrato, G.; Pitulescu, M. E.; Adams, R. H.; Parrinello, S., Direct cell-cell contact with the vascular niche maintains quiescent neural stem cells. *Nat Cell Biol* **2014,** 16, (11), 1045-56.
50. Luzzati, F.; Nato, G.; Oboti, L.; Vigna, E.; Rolando, C.; Armentano, M.; Bonfanti, L.; Fasolo, A.; Peretto, P., Quiescent neuronal progenitors are activated in the juvenile guinea pig lateral striatum and give rise to transient neurons. *Development* **2014,** 141, (21), 4065-75.
51. Paredes, M. F.; James, D.; Gil-Perotin, S.; Kim, H.; Cotter, J. A.; Ng, C.; Sandoval, K.; Rowitch, D. H.; Xu, D.; McQuillen, P. S.; Garcia-Verdugo, J. M.; Huang, E. J.; Alvarez-Buylla, A., Extensive migration of young neurons into the infant human frontal lobe. *Science* **2016,** 354, (6308).
52. Kempermann, G., A Back Door to Cortical Development. *Cell Stem Cell* **2017,** 20, (3), 295-296.

 doi:10.20944/preprints202106.0327.v1

53. Formaggio, E.; Fazzini, F.; Dalfini, A. C.; Di Chio, M.; Cantu, C.; Decimo, I.; Fiorini, Z.; Fumagalli, G.; Chiamulera, C., Nicotine increases the expression of neurotrophin receptor tyrosine kinase receptor A in basal forebrain cholinergic neurons. *Neuroscience* **2010,** 166, (2), 580-9.